

Full Characterization of a Strange Attractor

Chaotic Dynamics in Low-dimensional Replicator Systems

By

WOLFGANG SCHNABL, PETER F. STADLER, CHRISTIAN FORST

AND PETER SCHUSTER*

Institut für theoretische Chemie der Universität Wien

Mailing Address: Prof. Peter Schuster, Institut für theoretische Chemie
der Universität Wien

Währingerstraße 17, A 1090 Wien, Austria

Phone: (0222) 43 61 41 / 78 D

Bitnet: A8441DAM@AWIUNI11

Abstract

Two chaotic attractors observed in Lotka-Volterra equations of dimension $n = 3$ are shown to represent two different cross-sections of one and the same chaotic regime. The strange attractor is studied in the equivalent four dimensional catalytic replicator network. Analytical expressions are derived for the Ljapunov exponents of the flow. In the centre of the chaotic regime the strange attractor is characterized by numerically computed Rényi fractal dimensions, $D_q (q = 0, 1, 2) = 2.04, 1.89$ and 1.65 ± 0.05 as well as the Ljapunov dimension $D_L = 2.06 \pm 0.02$. Accordingly it represents a *multifractal*. The fractal set is characterized by the singularity spectrum.

Two routes in parameter space leading into the chaotic regime were studied in detail, one corresponding to the Feigenbaum cascade of bifurcations. The second route is substantially different from this well known pathway and has some features in common with the intermittency route. A series of one-dimensional maps is derived from a properly chosen Poincaré cross-section which illustrates structural changes in the attractor.

Mutations are included in the catalytic replicator network and the changes in the dynamics observed are compared with the predictions of an approach based on perturbation theory. The most striking result is the gradual disappearance of complex dynamics with increasing mutation rates.

1. Introduction

The search for chaotic dynamics became an issue in many scientific disciplines from physics to biology. The relevance of strange attractors in modeling real systems and the problem how to trace chaos in the experimental data were important questions already five years ago [1] and remained in the centre of interest since then [2-4]. Numerical evidence for strange attractors was found in many model equations but unlike simple attractors they cannot be characterized by a few coordinates or coordinates and frequencies. In the pioneering works of several groups efficient techniques to analyse chaotic dynamics and fractal sets were developed (For a recent review of the available repertoire of methods see [5,6]). In order to provide a sufficiently detailed basis for the comparison of model calculations and experimental data full characterization of strange attractors is required. We present such a study on a chaotic attractor which appears in the solutions of a differential equation which is of interest in biophysics and in theoretical ecology as well as in other disciplines.

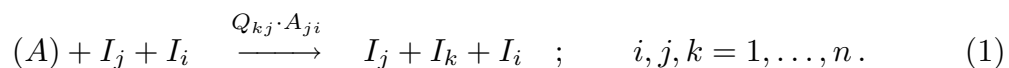
Autocatalytic reaction networks which involve two classes of catalytic processes – autocatalytic instruction for reproduction as well as material and process specific catalysis – were postulated as models for studies on prebiotic and early biological evolution scenarios [7,8]. Now they serve also as simple models showing the characteristic features of nonlinear dynamics in very different fields like molecular biology, population genetics, theoretical ecology or dynamical game theory [9].

Qualitative analysis and systematic numerical investigations revealed a very rich dynamics of the corresponding kinetic differential equations [10]. The name

replicator equations was coined for these systems because they reveal several unique and – in the standardized form to be discussed in the next section 2 – fairly easy to proof features [11]. The four species replicator system shows chaotic dynamics for certain parameter values [12]. According to Hofbauer [13] this autocatalytic network with four species is – apart from a transformation of the time scale – equivalent to a three-species Lotka-Volterra equation. Possible existence of very complex dynamical behaviour in Lotka-Volterra models was predicted by Smale [14]. Indeed two different strange attractors were reported for the Lotka-Volterra system [15-18], which describes communities of one predator species living on two prey species. In this contribution we shall show that the two strange attractors lie on different cross-sections through one and the same chaotic regime. The number of degrees of freedom is minimal for the occurrence of strange attractors and hence the chaotic regime in question houses the simplest strange attractors possible in Lotka-Volterra and replicator equations – replicator systems have normalized variables and hence the number of independent degrees of freedom is the number of species but one.

2. The replicator model

Replicator equations are based on the simplest possible molecular mechanism of catalysed replication and mutation. The basic reactions are of the form



Herein I_j is the template which is replicated and I_i the catalyst, (A) represents an overall notation for substrates needed for replication. It is assumed that the substrates are present in excess – their concentration are *buffered* and hence do not change during the course of reactions. There are n^3 possible reactions producing the n different species $I_k (k = 1, \dots, n)$ of the autocatalytic reaction network. Clearly it is very hard – if not impossible – to handle such a large number of parameters. In order to be able to analyse the reaction network simplifying assumptions are inevitable. It is straight forward to treat catalysed replication and mutation as independent superpositions: mutation frequencies depend on template (I_j) and target (I_k), but not on the catalyst (I_i). The remaining $2n^2$ rate parameters are properly understood then as elements of two $n \times n$ matrices: a replication rate matrix $A \doteq (A_{ji})$ and a mutation matrix $Q \doteq (Q_{kj})$. The rate constants of the individual reactions are products of a replication and a mutation factor. $Q_{kj} \cdot A_{ji}$, expressing the following sequence of processes: *I_i catalyzes the replication of I_j which yields I_k as an error copy.*

Error-free replication of species I_j – described by equ.(1) with $I_k \equiv I_j$ – is assumed to occur with frequency Q_{jj} . A mutation from I_j to $I_k, (k \neq j)$ occurs with frequency Q_{kj} . Every copy has to be either correct or a mutant and thus Q is a stochastic matrix ($\sum_{k=1}^n Q_{kj} = 1 \ \forall j = 1, \dots, n$).

Concentrations of individual species are denoted by $c_k = [I_k]$. As variables we use relative – or normalized – concentrations: $x_k = c_k / \sum_{j=1}^n c_j$ which obviously fulfil $\sum_{k=1}^n x_k = 1$.

Mass action kinetics applied to the autocatalytic reaction-mutation network

(1) yields an ODE of the form

$$\frac{dx_k}{dt} = \dot{x}_k = \sum_{i,j=1}^n Q_{ki} A_{ij} x_i x_j - x_k \Phi, \quad k = 1, \dots, n \quad (2)$$

where an automatically adjusted dilution flux

$$\Phi = \sum_{i,j=1}^n A_{ij} x_i x_j$$

is introduced in order to keep the sum of relative concentrations normalized to unity. The physically meaningful domain of equ.(2) is the simplex

$$S_n \doteq \left\{ (x_1, \dots, x_n) \mid x_i \geq 0, \sum_{i=1}^n x_i = 1 \right\}$$

If $A_{ij} \geq 0$, $i, j = 1, \dots, n$ then S_n is a compact, forward invariant set for the ODE (2).

An intensity of mutation can be measured by the *mean mutation rate* ϵ :

$$\epsilon \doteq \frac{1}{n(n-1)} \sum_{\substack{i \neq j \\ i,j=1}}^n Q_{ij} \quad (3)$$

Throughout this paper we use a particularly simple type of the mutation matrix

$$Q_{ij} = \begin{cases} 1 - (n-1)\epsilon, & \text{if } i = j; \\ \epsilon, & \text{if } i \neq j. \end{cases}$$

It represents a special case of the *house of cards* model of mutation [19,20] frequently used in theoretical population genetics.

The important special case of error-free replication is represented by a unit mutation matrix, $Q = id$. Then equ.(1) is turned into the well known *replicator equation*:

$$\dot{x}_k = x_k \left(\sum_{i=1}^n A_{ki} x_i - \sum_{i,j=1}^n A_{ij} x_i x_j \right) \quad (4)$$

The linear replicator equation (4) for n is flow-equivalent to the $n - 1$ species Lotka-Volterra equation:

$$\dot{y}_k = y_k \left(\alpha_k + \sum_{j=1}^{n-1} \beta_{kj} y_j \right) ; \quad k = 1, \dots, n - 1 . \quad (5)$$

The variables are related by means of the transformation introduced by Hofbauer [13]:

$$y_k = \frac{x_k}{x_n} \quad \text{for } k = 1, \dots, n - 1 . \quad (6)$$

3. The chaotic regime in parameter space

Two distinct chaotic attractors were found in Lotka-Volterra equations for three species: Vance [17] discovered a “quasi-cyclic” trajectory in a one predator two prey model and Arneodo, Couillet and Tresser [15] found a one parameter family of strange attractors (ACT-attractor). We used Hofbauer’s transform to construct the replicator equations which are equivalent to the models mentioned above. Then a barycentric transform [21] was applied to Vance’s model in order to shift the interior fixed point into the centre of the simplex S_4 – the point $\mathbf{c} = \frac{1}{4}(1, 1, 1, 1)$.

A barycentric transformation can always be found if the replicator equation

$$\dot{z}_k = z_k \left(\sum_{i=1}^n b_{ki} z_i - \sum_{i,j=1}^n b_{ij} z_i z_j \right)$$

has an interior fixed point $\hat{\mathbf{z}} = (\hat{z}_1, \hat{z}_2, \dots, \hat{z}_n)$. It can be shown [22] that there exists a *diffeomorphism* which relates this replicator equation to another one in the notation of equ.(4) with

$$A_{ij} = \frac{b_{ij}}{\hat{z}_j} \quad \text{and} \quad \hat{\mathbf{x}} = \frac{1}{n} (1, 1, \dots, 1) .$$

Both the ACT family and the Vance attractor (V) correspond to nonrobust phase-portraits because of zero or almost zero (see e.g. A_{24} or A_{43} in A_V) off-diagonal elements in the reaction matrices A . In order to make the numerical computations easy to reproduce all parameter values were rounded to three digits. Then the Vance model has a replication matrix

$$A_V = \begin{pmatrix} 0 & 0.063 & 0 & 0.437 \\ 0.537 & 0 & -0.036 & -0.001 \\ -0.535 & 0.38 & 0 & 0.655 \\ 0.536 & -0.032 & -0.004 & 0 \end{pmatrix} \quad (7)$$

and the ACT attractors are found at

$$A_{ACT} = \begin{pmatrix} 0 & 0.5 & -0.1 & 0.1 \\ 1.1 & 0 & -0.6 & 0 \\ -0.5 & 1 & 0 & 0 \\ 1.7 + \mu & -1 - \mu & -0.2 & 0 \end{pmatrix} \quad (8)$$

Note that we use a parameter μ which corresponds to $\mu - 1.5$ in [15].

In order to find out whether or not these two attractors are related in the twelve-dimensional parameter space we performed a systematic numerical survey

in the two-dimensional subspace (μ, ν) which connects the two models:

$$A(\mu, \nu) = \begin{pmatrix} 0 & 0.5 - 0.437\nu & -0.1 + 0.1\nu & 0.1 + 0.337\nu \\ 1.1 - 0.563\nu & 0 & -0.6 + 0.564\nu & -0.001\nu \\ -0.5 - 0.035\nu & 1 - 0.62\nu & 0 & 0.655\nu \\ 1.7 + \mu - 1.164\nu & -1 - \mu + 0.968\nu & -0.2 + 0.196\nu & 0 \end{pmatrix} \quad (9)$$

We note that all three matrices of replication constants fulfil $\sum_{j=1}^4 A_{ij} = 0.5 -$ a property which will be used together with the existence of a fixed point in the centre of the simplex later on.

In the (μ, ν) -plane the ACT model lies on the line $-0.2 \leq \mu \leq 0.05$ and $\nu = 0$. The Vance-attractor is close to the point $(0, 1)$. Both models are embedded in a Σ -shaped two-dimensional manifold of strange attractors (fig.1). In scanning through the manifold we could not find any sudden changes in the shape of the attractor. The mean revolution time also varies in apparently continuous manner all over the chaotic regime.

Fig. 1: A two-dimensional cross-section through the chaotic regime of equ.(4). The cross-section is defined by the two parameters μ and ν in the replication matrix A (9).

A common feature of all phase portraits exhibiting chaotic behaviour (attractive or only transient) is a saddle focus P_{123} on the $[1, 2, 3]$ -plane, which represents the stable manifold. The unstable manifold thus points into the interior of the simplex. We found that Šilnikov's condition [23] is always satisfied: the real positive eigenvalue is larger in magnitude than the real parts of the two complex

conjugate eigenvalues. Although there is no homoclinic orbit possible for P_{123} , a close relation to Šilnikov's condition is evident, as was pointed out by Arneodo *et al.* [16]: there is a heteroclinic orbit involving three saddles instead of one and this orbit replaces the homoclinic one. For generalized Lotka-Volterra models with additional cubic terms Samardzija and Greller [24] found a different type of chaos arising from a fractal torus.

For small values of μ the fixed point in the centre of S_4 (c) is stable. Chaos is reached via a Hopf bifurcation and a subsequent cascade of period doubling bifurcations. At first the limit cycle, and then the chaotic attractor, both grow steadily with increasing μ -values. At a parameter value around $\mu = 0.21$ the chaotic attractor collides with the stable manifold of a saddle on the $[1, 2, 4]$ -plane and disappears suddenly. This behaviour is known as *limit crisis* [25]: at the bifurcation point we find a heteroclinic orbit connecting the $[1, 4]$ -saddle, a saddle on the $[1, 2]$ -edge, and the saddle-focus in the $[1, 2, 3]$ -plane (fig.2). The evidence for the orbit is derived from numerical integration. We cannot provide an analytical proof for the saddle connection between the saddle focus and P_{12} . The saddle connections on the boundary follow from the invariance of the subsimplices and the classification of the flow of three component replicator equations [26,27].

Beyond the limit crisis we find a field of transient chaos: the trajectory seems to draw an image of the chaotic attractor which in parameter space lies on the other side of the limit crisis before it ends up in a stable fixed point.

For small values of ν the frequency of the oscillations increases with decreasing parameter values – revolution times become shorter and shorter. Eventually the

attractor collides with the stable manifold of the saddle on the $[1, 2]$ -edge. The invariant hyperplane $\sum_{k=1}^4 x_k = 1$ is a repeller in this area and therefore integration is extremely sensitive to numerical errors.

Fig. 2: A sketch of fourteen flows on the boundaries of the simplex S_4 which can coexist with the chaotic attractor in the interior. The numbers **(1)** to **(14)** are used as markers in fig.1 to indicate where the phase portraits occur in parameter space.

The chaotic attractor in the interior of the simplex S_4 coexists with a rather large variety of robust flows on the surface. Fig.2 shows fourteen boundary-flows consistent with chaos on the (μ, ν) -plane.

Fig.3 sketches the phase portraits of the ACT and the Vance model together with a typical chaotic trajectory for each system.

Fig. 3: Phase portraits and chaotic trajectories in the Vance (7) and the ACT model (8).

Direct evidence from the inspection of computed trajectories was supplemented by Fourier transformation [28]. Some typical examples of Fourier spectra in periodic and chaotic regimes of our attractor are shown in fig.4. They are used as a sensitive indicator of the occurrence of chaos. In the four spectra chosen we observe a complete transition from a periodic window into the chaotic regime caused by a small change in the parameters ($\Delta\mu < 0.02$).

Fig. 4: Fourier spectra of selected trajectories of the replicator model (9) with the parameter values $\nu = 0$ and $\mu = -0.0536$ (**A**), -0.0529 (**B**), -0.05 (**C**) and -0.04 (**D**).

4. Measures of the chaotic attractors

The most common measure for a chaotic attractor is the spectrum of Ljapunov exponents [29]. Let $J(t) = \partial \mathcal{F}(\mathbf{x}(\mathbf{x}(0), t))$ be the Jacobian of the vectorfield \mathcal{F} along a trajectory with starting point $\mathbf{x}(0)$. Now we define an operator

$$\mathcal{L}(t) \doteq \hat{\mathbf{T}} \left\{ \exp \int_0^t J(\tau) d\tau \right\}. \quad (10)$$

The *time ordering operator* $\hat{\mathbf{T}}$ has to be introduced since Jacobian matrices evaluated at different times – $J(\tau)$ and $J(\tau')$ – usually do not commute. Let $\mu_i(t)$ be the eigenvalues of $\mathcal{L}(t)$, then the Ljapunov exponents are given by

$$\lambda_i = \lim_{t \rightarrow \infty} \frac{\ln \|\mu_i(t)\|}{t}. \quad (11)$$

In most cases it is not possible to calculate Ljapunov exponents for the flows of differential equations analytically. An appropriate numerical algorithm has been given by Bennetin *et al.* [30], a well tested FORTRAN program is available in the literature [31].

In the four-species replicator system there are three physical dimensions imbedded in a four-dimensional state space. The hyperplane

$$\Sigma_4 = \left\{ \mathbf{x} \in \mathbb{R}^4 \mid \sum_{i=1}^4 x_i = 1 \right\}$$

is invariant. Accordingly $\mathcal{L}(t)$ has three eigenvectors $\vec{\xi}_i$ lying in this plane and their components fulfil $\sum_k \xi_k^{(i)} = 0$. The fourth eigenvector is pointing out of the hyperplane. Thus we expect to find three physical meaningful Ljapunov exponents. If all three of them are negative the attractor is a sink. For a periodic, quasiperiodic or chaotic attractor at least one eigenvalue has to be zero: this exponent corresponds to an eigenvector which points in the direction of the trajectory. In particular, we have for periodic orbits $\lambda_1 \leq \lambda_2 < 0, \lambda_3 = 0$, for quasiperiodic orbits $\lambda_1 < 0, \lambda_2 = \lambda_3 = 0$ and finally for a chaotic attractor one Ljapunov exponent is negativ, one is zero and one is positiv, $\lambda_1 < 0, \lambda_2 = 0, \lambda_3 > 0$. The sum of all Ljapunov exponents fulfils the equation

$$\sum_{i=1}^n \lambda_i = \lim_{t \rightarrow \infty} \frac{1}{t} \int_0^t \operatorname{div} \mathcal{F}(\mathbf{x}(\tau)) d\tau \quad (12)$$

For error-free replication – if the mutation matrix $Q = id$ – the divergence $\operatorname{div} \mathcal{F}$ reduces to

$$\operatorname{div} \mathcal{F} = \sum_{k,j=1}^n A_{kj} x_j - (n+2) \sum_{i,j=1}^n A_{ij} x_i x_j . \quad (13)$$

The mean flux $\bar{\Phi}$ is defined by

$$\bar{\Phi} = \lim_{t \rightarrow \infty} \frac{1}{t} \int_0^t \sum_{i,j=1}^n A_{ij} x_i(\tau) x_j(\tau) d\tau$$

If the replicator equation is permanent [11,32,33] – or at least if the trajectory converges to an interior fixed point – we have

$$\begin{aligned} 0 &= \lim_{t \rightarrow \infty} \frac{1}{t} \int_0^t \frac{\dot{x}_k}{x_k} d\tau = \lim_{t \rightarrow \infty} \frac{1}{t} \left\{ \frac{\log x_k(t) - \log x_k(0)}{t} \right\} = \\ &= \sum_{j=1}^n A_{kj} \lim_{t \rightarrow \infty} \frac{1}{t} \int_0^t x_j(\tau) d\tau - \lim_{t \rightarrow \infty} \frac{1}{t} \int_0^t \sum_{i,j=1}^n A_{ij} x_i(\tau) x_j(\tau) d\tau = \\ &= \sum_{j=1}^n A_{kj} \bar{x}_j - \bar{\Phi} \end{aligned}$$

Since the last line is the equation fulfilled by the coordinates of the interior fixed point we have

$$\bar{x}_j = \lim_{t \rightarrow \infty} \frac{1}{t} \int_0^t x_j(\tau) d\tau = \hat{x}_j \quad (14)$$

where $\hat{\mathbf{x}} = (\hat{x}_1, \hat{x}_2, \dots, \hat{x}_n)$ is the interior fixed point if it exists. Its coordinates fulfil the equations

$$\sum_j^n A_{ij} \hat{x}_j = \bar{\Phi} ,$$

and hence we have

$$\sum_{i,j=1}^n A_{ij} \hat{x}_j = n \cdot \bar{\Phi} \quad \forall \quad i = 1, \dots, n .$$

Accordingly we find

$$\lim_{t \rightarrow \infty} \frac{1}{t} \int_0^t \operatorname{div} \mathcal{F}(\mathbf{x}(\tau)) d\tau = -2 \cdot \bar{\Phi} . \quad (15)$$

Finally we are left with the following relation derived from equ.(12) for the sum

$$\sum_{i=1}^n \lambda_i = -\frac{2}{n^2} \sum_{i,j=1}^n A_{ij} . \quad (12a)$$

Since we applied the *barycentric* transformation to our model, $\hat{x}_j = \frac{1}{n}$ holds for all coordinates and we obtain

$$\bar{\Phi} = \frac{1}{n^2} \sum_{i,j=1}^n A_{ij} .$$

Using the numerical values of (9) the sum of the four Ljapunov exponents becomes $\sum_{i=1}^4 \lambda_i = -\frac{1}{4}$. The eigenvector pointing in the direction (1, 1, 1, 1) is denoted by

$$\mathbf{e} = \frac{1}{2} \begin{pmatrix} 1 \\ 1 \\ 1 \\ 1 \end{pmatrix}$$

The corresponding Ljapunov exponent (λ_4) can be calculated analytically. Let us consider the orbit of the linearized model starting from $\mathbf{x}(0) = \mathbf{e}$ which to first order in time is given by

$$\mathbf{x}(\tau) = \mathbf{e} + \tau \cdot \partial \mathcal{F} \cdot \mathbf{e} + O(\tau^2) .$$

Then we obtain for the Ljapunov exponent

$$\begin{aligned} \lambda_4 &= \lim_{N \rightarrow \infty} \lim_{\tau \rightarrow 0} \frac{1}{N\tau} \sum_{j=1}^N \log\{\tau \cdot \langle \mathbf{e} | I + \partial \mathcal{F}(\mathbf{x}(j\tau)) | \mathbf{e} \rangle\} = \\ &= \lim_{N \rightarrow \infty} \lim_{\tau \rightarrow 0} \frac{1}{N\tau} \sum_{j=1}^N \tau \cdot \langle \mathbf{e} | \partial \mathcal{F}(\mathbf{x}(j\tau)) | \mathbf{e} \rangle = \\ &= \lim_{t \rightarrow \infty} \frac{1}{t} \int_0^t \langle \mathbf{e} | \partial \mathcal{F}(\mathbf{x}(\tau)) | \mathbf{e} \rangle d\tau = -\bar{\Phi} \end{aligned}$$

The last equation is derived straightway by explicit evaluation of the integrand as the sum over all elements of the Jacobian. One obtains the same result $-\Phi(\tau)$ for every time τ and hence $\lambda_4 = -\bar{\Phi}$.

Thus we have in case of our model:

$$\sum_{i=1}^4 \lambda_i = -\frac{1}{4} \quad \text{and} \quad \lambda_4 = -\frac{1}{8} . \quad (16)$$

In the chaotic regime it is sufficient therefore to compute the largest Ljapunov exponent λ_1 . All other exponents are obtained from:

$$\lambda_2 = 0, \quad \lambda_3 = -\frac{1}{8} - \lambda_1 \quad \text{and} \quad \lambda_4 = -\frac{1}{8} . \quad (17)$$

In fig.5 we show the largest Ljapunov exponent (λ_1) of the strange attractor as a function of the parameter μ .

Fig. 5: The largest Ljapunov exponent λ_1 of the vector flow defined by equ.(9). In order to show a representative cross-section through the chaotic regime we chose $\nu = 0$.

From the Ljapunov exponents we can calculate an estimate for the fractal dimension of our attractor:

$$D_L = \begin{cases} 2 - \frac{\lambda_1}{\lambda_3} = 2 \left(\frac{1 + 12\lambda_1}{1 + 8\lambda_1} \right) & \text{if } \lambda_1 > 0, \\ 1 & \text{if } \lambda_1 = 0 \text{ and} \\ 0 & \text{if } \lambda_1 < 0. \end{cases} \quad (18)$$

From fig.5 we obtain $\lambda_1 = 8 \times 10^{-3}$ for the highly developed chaos at $\mu = \nu = 0$ and compute a dimension of $D_L = 2.06$ with an estimated numerical uncertainty of ± 0.02 at this point.

In order to study the fractal nature of the attractor quantitatively we computed also generalized or Rényi dimensions, D_q , which correspond to the scaling exponents of the q -th moments of the attractor's measure [34,35]. The attractor is covered by $M(\ell)$ cells with edges of length ℓ . By p_i we denote the probability to find a point of the attractor in cell number i ($i = 1, \dots, M(\ell)$). Then Rényi dimensions are obtained from

$$D_q = \lim_{\ell \rightarrow 0} \frac{\log \sum_{i=1}^{M(\ell)} p_i^q}{(q-1) \log \ell} = \lim_{\ell \rightarrow 0} \frac{\log C^q(\ell)}{(q-1) \log \ell}, \quad (19)$$

where we introduced the definition $C^q(\ell) \doteq \sum_{i=1}^{M(\ell)} p_i^q$. In order to circumvent an indeterminate expression in the denominator the Rényi dimension D_1 is obtained by taking the limit $\lim_{q \rightarrow 1} D_q = D_1$. For the actual calculations we can rewrite

the sum over the p_i 's in terms of the probability \tilde{p}_i of the trajectory to cross a box of size ℓ around the iterate $x(t_j)$. We make use of the equation

$$\lim_{\ell \rightarrow 0} \sum_{i=1}^{M(\ell)} p_i^q = \lim_{N \rightarrow \infty} \frac{1}{N} \sum_{j=1}^N \tilde{p}_j^{q-1} \quad (20)$$

and find that the latter probability is given by

$$\tilde{p}_j = \lim_{N \rightarrow \infty} \frac{1}{N} \sum_{i=1}^N \Theta(\ell - \|\mathbf{x}_i - \mathbf{x}_j\|) , \quad (21)$$

where Θ is used for the *Heaviside function*:

$$\Theta(x - x_0) = \begin{cases} 0 & \text{for } x < x_0 , \\ 1 & \text{for } x \geq x_0 . \end{cases}$$

Thus we are left with the easier to compute expression

$$C^q(\ell) = \lim_{N \rightarrow \infty} \frac{1}{N^q} \sum_{j=1}^{M(\ell)} \left(\sum_{i=1}^{M(\ell)} \Theta(\ell - \|\mathbf{x}_i - \mathbf{x}_j\|) \right)^{q-1} . \quad (22)$$

In the limit $q \rightarrow 1$ we find for the Rényi dimension

$$D_1 = \lim_{N \rightarrow \infty} \lim_{\ell \rightarrow 0} \frac{1}{N \cdot \log \ell} \sum_{j=1}^N \log \left(\frac{1}{N} \sum_{i=1}^N \Theta(\ell - \|\mathbf{x}_i - \mathbf{x}_j\|) \right) . \quad (23)$$

For the lowest integer q values the Rényi dimensions D_q are equal to Hausdorff dimensions ($q = 0$), information dimensions ($q = 1$) and correlation dimensions ($q = 2$).

The evaluation of Rényi dimensions turned out to be extremely time consuming and therefore we restricted computations to one point right in the centre of the chaotic regime ($\mu = \nu = 0$). In order to calculate the numbers $C^q(\ell)$ the trajectory was decomposed into a time series

$$\mathbf{X} = \{ \mathbf{X}_i = \mathbf{x}(t_i) \mid \forall i = 1, 2, \dots, N \} \quad (24)$$

with $t_1 < t_2 < \dots < t_N$. Some ten thousand points are required which have to be distributed *independently* along a trajectory. This condition can be met by collecting subsequent points which are separated by at least one full revolution on the attractor. We record mean revolutions times of the order $t_R \approx 10^2$ for our attractor and hence the trajectory had to be followed up to $t \approx 2 \times 10^5$. Inserting the fractal set obtained into eqs.(22) and (23) we found

$$D_0 = 2.04, \quad D_1 = 1.89 \quad \text{and} \quad D_2 = 1.65.$$

The estimated numerical uncertainty of our values amounts to ± 0.05 . We note that the Hausdorff dimension of the attractor is the same as the Ljapunov dimension within the error limits and fulfils the condition $D_L \geq D_0$.

Fractal sets can be characterized by the scaling properties of normalized distributions or *measures* lying upon them [36]. We briefly repeat the basic expressions and relations. Scaling properties are expressed in terms of singularity strengths α and a function $f(\alpha)$ which reflects the density of their distribution. The *spectrum* of singularities is given by the possible range of α values and the density $f(\alpha)$. In order to define these quantities we cover the attractor with boxes of size ℓ and denote the number of points inside the i th box by N_i . Then the probability that this box contains a point of the attractor's time series (24) is given by $P_i(\ell) = \lim_{N \rightarrow \infty} (N_i / N)$. The local singularity strength α_i is now given as the scaling exponent $P_i(\ell) \propto \ell^{\alpha_i}$. The singularity strength α_i thus varies with the region of the attractor on which it is taken. Its probability density - the probability to encounter a value of α between $\tilde{\alpha}$ and $\tilde{\alpha} + d\tilde{\alpha}$ - is given by

$$\text{Prob} \{ \tilde{\alpha} < \alpha < \tilde{\alpha} + d\tilde{\alpha} \} = d\alpha \rho(\alpha) \ell^{-f(\tilde{\alpha})}$$

where $f(\alpha)$ is a continuous function. The set of singularity strengths α_i itself is a fractal and $f(\alpha)$ can be understood as its – fractal – dimension. In other words, fractal measures are modeled by interwoven sets of singularities of strength α – each one having its own fractal dimension $f(\alpha)$.

The singularity spectrum $f(\alpha)$ is related to the Rényi dimensions D_q since

$$C^q(\ell) = C(q, \ell) = \int d\tilde{\alpha} \rho(\tilde{\alpha}) \ell^{q\tilde{\alpha}} \ell^{-f(\tilde{\alpha})} .$$

The dimensions are defined in the limit $\ell \rightarrow 0$ and accordingly we may approximate the integral for nonzero densities $\rho(\tilde{\alpha})$ by the term with the smallest exponent $q\tilde{\alpha} - f(\tilde{\alpha})$. This value $\alpha(q)$ is defined by

$$\left. \frac{d}{d\tilde{\alpha}} (q\tilde{\alpha} - f(\tilde{\alpha})) \right|_{\tilde{\alpha}=\alpha(q)} = 0$$

and the existence of a minimum requires

$$\left. \frac{d^2}{d(\tilde{\alpha})^2} (q\tilde{\alpha} - f(\tilde{\alpha})) \right|_{\tilde{\alpha}=\alpha(q)} > 0$$

which finally yields $f'(\alpha(q)) = q$ and $f''(\alpha(q)) < 0$. We have two relations

$$D_q = \frac{1}{q-1} [q\alpha(q) - f(\alpha(q))] \quad \text{and} \quad \alpha(q) = \frac{d}{dq} ((q-1)D_q) \quad (25)$$

which allow two compute the singularity spectrum from known Rényi dimension or vice versa. It can be shown straightway that the Hausdorff dimension of the attractor fulfils $D_0 = f(\alpha_{\max})$ where α_{\max} is the position of the maximum of $f(\alpha)$.

Feigenbaum [37] recently pointed out that this formalism is related to the thermodynamic formalism of equilibrium statistical mechanics. A new function

$\tau(q) \doteq (q-1)D_q$ is introduced. The singularity spectrum $f(\alpha)$ is the Legendre transform of τ . In Feigenbaum's formalism $\tau(q)$ and q are conjugate thermodynamic variables to $f(\alpha)$ and D_q .

Fig. 6: The singularity spectrum of the strange attractor in the centre of the chaotic regime ($\mu = 0, \nu = 0$). Note that the maximum of $f(\alpha)$ represents the Hausdorff dimension (D_0) of the attractor.

The singularity spectrum of the strange attractor with $\mu = \nu = 0$ was calculated from a series of Rényi dimensions. For a given set of values $q = q_k$ the singularity strenghts were obtained by partial differentiation: $\alpha(q) = \frac{\partial \tau}{\partial q}$. The partial derivatives were computed by means of a five point differentiation formula. Then we derived $f(\alpha)$ for discrete points $\alpha_k = \alpha(q_k)$ from

$$f(\alpha_k) \doteq f_k = \alpha_k q_k - (q_k - 1)D_{q_k} . \quad (26)$$

Limiting dimensions can be derived straightway from the singularity spectrum: $D_{+\infty} = \alpha(q = +\infty)$ and $D_{-\infty} = \alpha(q = -\infty)$. Both limits are related to the singularity spectrum by $f(\alpha(q = \pm\infty)) = 0$. In the case of our chaotic attractor we find $1.3 \leq \alpha \leq 3$. This result can be interpreted as follows: in case the trajectory visits a volume element in the three dimensional concentration simplex S_4 , it occupies a fractal set whose measure has a Hausdorff dimension of $\alpha \approx 1.3$ or larger. For larger negative values of q the estimates of the Rényi dimensions are rather poor, because the limit in equ.(22) converges very slowly. Thus the right hand branches of the computed singularity spectra are inaccurate and we expect rather

large errors for the extrapolated values of $D_{-\infty}$. Indeed straight extrapolation of the points obtained would yield an upper limit around 3.5 (fig.6). It can be expected, however, that the correct upper limit is $\alpha = 3$ since the trajectory is ultimately restricted to the simplex S_4 .

5. The routes to chaos

Routes into chaotic dynamics were studied by means of Poincaré maps in the plane defined by $x_4 = \frac{1}{4}$. Distributions of points at which a long-time trajectory crosses this plane are shown in fig.7. A Cartesian coordinate system is defined with the origin in the central fixed point $\mathbf{c} = \frac{1}{4}(1, 1, 1, 1)$ (fig.7) and the branch starting near \mathbf{c} and extending towards the projection of the [1,2]-edge onto the plane $x_4 = \frac{1}{4}$ is chosen as Poincaré cross-section. Its shape is very close to a straight line.

Fig. 7: Points at which a long-time trajectory crosses the plane $x_4 = \frac{1}{4}$. Orientation of the attractor relative to the cross-section and three examples with $\nu=0$ and $\mu = -0.2, 0$ and 0.1 are shown.

Time series $\Xi = (\Xi_1, \Xi_2, \dots, \Xi_N)$ are defined as successive points at which the trajectory passes the Poincaré cross-section. They were recorded as a function of the parameter μ ($-0.21 < \mu < 0.21$) with the second parameter held constant at the value of the ACT model ($\nu=0$). The corresponding plot is shown in fig.8. The

first part ($-0.21 < \mu < -0.01$) reminds of the analogous plot of the discrete logistic map on the unit interval: $X_{n+1} = r \cdot X_n(1 - X_n)$. Indeed there is a monotonous – almost linear – relation between the values of the constant r and the parameter μ at which the characteristic period doublings and periodic windows in the chaotic regime occur (fig.9). The sequence of events into chaos and the structure of the chaotic regime along this route show perfect correspondence to the well known Feigenbaum sequence. A more precise characterization of the individual periodic regimes is contained in table 1.

Fig. 8: A Poincaré map of the attractors with $\nu=0$ as a function of the parameter μ . A projection of the Poincaré map onto the y -axis defined in fig.7 is shown. The origin coincides with the centre of the fixed point **C**.

Fig. 9: Relation between the critical values of the parameter r in Feigenbaum's sequence of bifurcations and periodic windows in the chaotic regime of the logistic map on the unit interval and the values of the parameter μ at which the analogous events occur in the dynamics of the replicator equation.

As in the logistic map, the range on the Poincaré section which is visited by the chaotic trajectory grows with increasing values of the parameter μ . In contrast to the former, however a certain region around the central fixed point **c** is always left blanc. Beyond the end of the Feigenbaum sequence we observe a broad continuation of the chaotic regime up to a sharp interior crisis at $\mu \approx 0.045$. Characteristic accumulation zones of points on the cross-section which continue as

Table 1: Periodic windows in the chaotic regime ($-0.105 < \mu < 0.1684$).[†]

Period [‡]	Range of μ values		Comments
	begin	end	
12	-0.1034		Begin of Feigenbaum sequence
6	-0.0956	-0.0948	
5	-0.0770	-0.760	
10	-0.0632		
3 ff.	-0.0587	-0.0527	
5	-0.0398		
7	-0.0359		
6	-0.0326		
4 ff.	-0.0255	-0.0250	
6	-0.0182		
7	-0.0116		End of Feigenbaum sequence
9	0.0082		
3 ff.	0.0118	0.0127	
4	0.0227		
6	0.0448		Interior crisis
2 ff.	0.0544	0.0772	
12	0.0784		
7	0.0844		
12	0.0865	0.0868	
8 ff.	0.0883	0.0892	
4	0.0922	0.0980	
6	0.1057	0.1060	
12	0.1090		
6	0.1102		
2 ff.	0.1207	0.1291	
6	0.1312		
10	0.1489		
4	0.1543		

[†] In the case of very narrow windows only one parameter value is given.[‡] Windows in which at least one period doubling event was identified are indicated by “ff.”.

Table 2: Chaotic windows in the essentially periodic regime (Period 2 in the range $0.1684 < \mu < 0.2085$).[†]

Range of μ values	
begin	end
0.1687	0.1690
0.1714	
0.1801	0.1807
0.1822	0.1828
0.1873	0.1891
0.1945	0.1954
0.1981	0.1993
0.2029	
0.2041	
0.2062	
0.2074	0.2081

[†] In the case of very narrow windows only one parameter value is given.

lines through periodic windows appear in the range above $\mu \approx -0.01$ as well. They look as if they were reflected at the lower boundary of the chaotic regime near the point **c**.

At μ values above the interior crisis we observe a second period doubling cascade ending in small chaotic regime which is again interrupted by periodic windows. Chaos expands with increasing μ -values and eventually ends abruptly at a limit crisis around $\mu \approx 0.17$. Beyond the second crisis we observe in essence a double periodic regime interrupted by small windows with significantly positive Ljapunov exponents. The chaotic windows at parameter values $\mu < 0.16$ are summarized in table 2.

Approaching the chaotic regime from high to low values of μ we observe a

periodic attractor appearing first at $\mu \approx 0.21$. This attractor changes – at some points discontinuously – and small chaotic windows occur in the periodic regime which remind of intermittence. Eventually chaos is reached in one step at $\mu \approx 0.17$.

Fig. 10: Return maps on the unit interval corresponding to the Poincaré cross-section for different parameter values ($\nu=0$).

A: $\mu = -0.101$, **B:** $\mu = -0.029$, **C:** $\mu = -0.002$, **D:** $\mu = 0.016$,
E: $\mu = 0.088$ and **F:** $\mu = 0.142$.

For few selected values of the parameter μ we constructed return maps on the unit interval which are shown in fig.10. As expected the maps resemble closely the logistic map in the parameter range where we observe the Feigenbaum sequence. At higher values of μ the map becomes more sophisticated and a second maximum appears.

6. Mutation caused changes in the chaotic regime

Mutation is an *unavoidable* by-product of replication. Quantitative answers to the questions if and how complex dynamics is changing under the influence of mutation is of obvious importance for biological applications. Therefore we performed a study of the influence of mutation on the chaotic attractor in the replicator equation. Equ.(2) with rate constants A_{ij} according to (9) was studied by a version of perturbation theory [38] under the simplifying assumption of equal mutation rates ($Q_{ij} = \epsilon$ for $i \neq j$; equ.(3) shows the definition of ϵ). The kinetic

equations for replication and mutation are rewritten in such a way that error-free production and mutant formation appear as additive contributions:

$$\dot{\mathbf{x}} = \mathcal{R}(\mathbf{x}) + \mathcal{M}(\mathbf{x}, \epsilon) \quad (27)$$

$$\text{with} \quad \mathcal{R}_k = x_k \left(\sum_j A_{kj} x_j - \sum_{i,j} A_{ij} x_i x_j \right) \quad \text{and}$$

$$\mathcal{M}_k = \sum_{i,j} \left(Q_{ki}(\epsilon) A_{ij} x_i x_j - Q_{ik}(\epsilon) A_{kj} x_k x_j \right) .$$

The first part – the unperturbed equation – is identical with equ.(4). Mutation \mathcal{M} is considered as perturbation with ϵ being the perturbation parameter. The replicator part is insensitive to the addition of constants to the reaction rate parameters: $A_{ij} \rightarrow A_{ij} + \Delta$ [39]. In order to make the perturbation approach applicable to equ.(9) we had to apply a sufficiently large value of this additive constant which was chosen to be $\Delta=8$.

The influence of mutation on the position of the k th fixed point of the unperturbed replicator equation (4) ($\mathbf{x}_k^{(0)}$) is expressed by

$$\mathbf{x}_k(\epsilon) = \mathbf{x}_k^{(0)} + \epsilon \cdot \mathbf{d}_k + O(\epsilon^2) . \quad (28)$$

As shown in [38] the shift \mathbf{d}_k is obtained from

$$J(\mathbf{x}_k^{(0)}) \cdot \mathbf{d}_k = -\mathcal{M}(\mathbf{x}_k^{(0)}) , \quad (29)$$

where $J(\mathbf{x})$ represents the Jacobian of the unperturbed system: $J_{ij} = \frac{\partial \mathcal{R}_i}{\partial x_j}$. In table 3 we summarize the shifts of all important fixed points of our model replicator equation determined by (9).

Table 3: Shifts of individual fixed points caused by mutation in the replicator model (9). All mutation rate were assumed to be equal ($Q_{ij} = \epsilon \forall i \neq j$) and the results were obtained by means of perturbation theory [38].

k^\dagger	Fixed point $\mathbf{x}_k^{(0)}$	Shift vector \mathbf{d}_k
1	$\begin{pmatrix} 1 \\ 0 \\ 0 \\ 0 \end{pmatrix}$	$\frac{16}{11(10\mu+17)} \cdot \begin{pmatrix} -(60\mu+47) \\ -5(10\mu+17) \\ 11(10\mu+17) \\ 55 \end{pmatrix}$
2	$\begin{pmatrix} 0 \\ 1 \\ 0 \\ 0 \end{pmatrix}$	$\frac{8}{1+\mu} \cdot \begin{pmatrix} -2(\mu+1) \\ 3\mu+2 \\ \mu+17 \\ 1 \end{pmatrix}$
3	$\begin{pmatrix} 0 \\ 0 \\ 1 \\ 0 \end{pmatrix}$	$\frac{40}{3} \cdot \begin{pmatrix} 6 \\ 1 \\ -10 \\ 3 \end{pmatrix}$
12	$\frac{1}{16} \begin{pmatrix} 5 \\ 11 \\ 0 \\ 0 \end{pmatrix}$	$\frac{89}{176(3\mu+4)} \cdot \begin{pmatrix} 18\mu+13 \\ 219\mu+181 \\ -88(3\mu+4) \\ 132 \end{pmatrix}$
13	$\frac{1}{6} \begin{pmatrix} 1 \\ 0 \\ 5 \\ 0 \end{pmatrix}$	$\frac{95}{42(5\mu+6)} \cdot \begin{pmatrix} -90\mu-73 \\ 5(5\mu+6) \\ 15\mu+88 \\ -105 \end{pmatrix}$
14	$\frac{1}{2(5\mu+9)} \begin{pmatrix} 1 \\ 0 \\ 0 \\ 10\mu+17 \end{pmatrix}$	$\frac{810\mu+1457}{(5\mu+3)(5\mu+9)(5\mu+11)(10\mu+17)} \cdot \begin{pmatrix} (5\mu+11)(100\mu^2+265\mu+167) \\ (5\mu+9)(5\mu+11)(10\mu+17) \\ (5\mu+3)(5\mu+9)(10\mu+17) \\ 1000\mu^3+4875\mu^2+7730\mu+3979 \end{pmatrix}$
123	$\frac{1}{32} \begin{pmatrix} 10 \\ 7 \\ 15 \\ 0 \end{pmatrix}$	$\frac{43}{112(3\mu+5)} \cdot \begin{pmatrix} -6(9\mu-13) \\ 87\mu+61 \\ -33\mu+533 \\ 672 \end{pmatrix}$

Table 3: Continuation

k^\dagger	Fixed point $\mathbf{x}_k^{(0)}$	Shift vector \mathbf{d}_k
124	$\frac{1}{8(5\mu+6)} \begin{pmatrix} 5\mu+5 \\ 5\mu+3 \\ 0 \\ 10(3\mu+4) \end{pmatrix}$	$\frac{651\mu+779}{(\mu+1)(3\mu+4)(3\mu+5)(5\mu+3)(5\mu+6)} \cdot \begin{pmatrix} (\mu+1)(5\mu+7)(30\mu^2+25\mu-31) \\ 150\mu^4+395\mu^3-55\mu^2-767\mu-459 \\ (\mu+1)(3\mu+4)(5\mu+3)(5\mu+6) \\ 150\mu^4+530\mu^3+544\mu^2+65\mu-97 \end{pmatrix}$
134	$\frac{1}{2(5\mu+9)} \begin{pmatrix} 1 \\ 0 \\ 5\mu+11 \\ 5\mu+6 \end{pmatrix}$	$\frac{160\mu+287}{(3\mu+5)(5\mu+6)(5\mu+9)(5\mu+11)} \cdot \begin{pmatrix} (5\mu+11)(100\mu^2+265\mu+167) \\ (5\mu+6)(5\mu+9)(5\mu+11) \\ 1875\mu^4+13125\mu^3+33825\mu^2+37815\mu+15392 \\ 1875\mu^4+13750\mu^3+36900\mu^2+42660\mu+17823 \end{pmatrix}$

[†] The individual fixed points are denoted by indicating the nonvanishing coordinates as subscript. The fixed point $\mathbf{x}_4^{(0)}$ is non-hyperbolic – its Jacobian has one zero eigenvalue – and hence cannot be subjected to the analysis presented here. All other fixed points not included in the table lie outside the simplex S_4 .

Fig.11 summarizes the changes in the chaotic attractor due to mutation. The main result of our study is that – at least this particular type of – chaotic dynamics is very sensitive to mutation: mutation probabilities as small as 2×10^{-5} are sufficient to destroy the strange attractor. At higher mutation rates – ϵ larger than some 10^{-3} – the interior fixed point is stable. A decrease in the mutation rate leads to a sequence of period doublings which eventually ends up in chaos. A highly complex bifurcation structure arises on the introduction of mutation near

the limit crisis of the unperturbed attractor. Fig.12 shows an enlarged portion of fig.11 with a resolution of approximately 0.005 in μ and 5×10^{-7} in ϵ . At the present stage of resolution we cannot say whether the bifurcation set forms a fractal or not.

Fig. 11: Extension of the chaotic regime into the range of small mutation rates.

Fig. 12: An enlargement of the bifurcation diagram near the limit crises of the unperturbed replicator equation.

It is not surprising that even small mutation rates destroy the chaotic attractor since the mutation term causes the saddle focus to move into the unphysical range outside of the simplex S_4 [38]. Therefore the trajectories can no longer come sufficiently close to the saddle and Šilnikov's mechanism breaks down. Furthermore the fixed point P_{12} moves into the interior of S_4 and thus the limit crisis occurs earlier.

7. Conclusions

The strange attractor in Lotka-Volterra and replicator systems of low dimension was fully characterized in a two-dimensional subspace of the twelve-dimensional parameter space. We were able to show that both chaotic attractors reported for these dynamical systems so far, lie within the same chaotic regime.

There is no doubt that this regime extends also into other directions in parameter space. Because of technical limitations we have to leave the systematic multi-dimensional search as a project for the future. Still unanswered is also the question whether or not other chaotic regimes exist in areas which are not connected to the investigated one.

One cross-section through the chaotic regime was studied in great detail. Along this path chaos developes in an almost perfect *Feigenbaum scenario* and then it breaks down in several interior crises – a major one and a few minor events – and ends in the final limit crisis. On further continuation along the path one encounters a periodic regime with is intermitted by a few, very small chaotic windows. The chaos is never fully developed: a small hole around the central – unstable – fixed point remains always left out by the long-time trajectories. Right in the centre of the chaotic regime the fractal set produced by the attractor is of multi-fractal type. The distribution of dimensions covers a range from 1.3 to 3.

The replicator equation allows straight inclusion of mutation which inevitably occurs in nature. The most relevant result we obtained in the present study is a substantial reduction in the dynamical *complexity* with increasing mutation rates. Strange attractors are replaced by stable closed orbits, limit cycles are converted into stable attractors. It is interesting to note that we found a Feigenbaum sequence in opposite direction: reduction of the error-rate yields a cascade of bifurcations which eventually ends in the chaotic attractor of the unperturbed system. We cannot claim – nor do we intend to – that increased mutation will always leads

to simpler dynamics but general intuition favours this view: mutation can be understood as a *force* pushing trajectories towards the centre of the concentration simplex. Wide *excursions* of trajectories which are characteristic for sophisticated closed orbits and strange attractors are less likely if the attractor lives near the centre.

Acknowledgements

Financial support was provided by the Austrian *Fonds zur Förderung der wissenschaftlichen Forschung* (Project No.6864) and by the *Stiftung Volkswagenwerk* (B.R.D.). Stimulating discussions with Prof.Dr.Harald Posch are gratefully acknowledged. This work required extensive use of computers and we are particularly grateful for generous supply with CPU time at the *IBM 3090-400 VF* mainframe computer of the *EDV-Zentrum der Universität Wien* within the *EASI* project of IBM and at the *NAS 9160* mainframe computer of the *IEZ Wien*.

References

- [1] P.E.Kloeden and A.I.Mees, *Bull.Math.Biol.***47**(1985) 697.
- [2] A.Chhabra and R.V.Jensen, *Phys.Rev.Lett.***62**(1989) 1327.
- [3] A.M.Fraser, *Physica* **34D**(1989) 391.
- [4] E.Gutierrez and H.Almirall, *Bull.Math.Biol.***51**(1989) 785.
- [5] H.G.Schuster, *Deterministic chaos – an introduction* 2nd Ed.,
VCh-Verlagsges., Weinheim (B.R.D.) 1988.
- [6] R.W.Leven, B.-P.Koch and B.Pompe, *Chaos in dissipativen Systemen*
F.Vieweg & Sohn, Braunschweig (B.R.D.) 1989.
- [7] M.Eigen, *Naturwissenschaften* **58**(1971) 465.
- [8] M.Eigen and P.Schuster, *The hypercycle – a principle of natural self-
organization*. Springer-Verlag, Berlin 1979.
- [9] P.Schuster and K.Sigmund, *J.Theor.Biol.***100**(1983) 533.
- [10] P.Schuster, *Physica* **22D**(1986) 100.
- [11] J.Hofbauer and K.Sigmund, *The theory of evolution and dynamical systems
– mathematical aspects of selection*. Cambridge University Press, Cam-
bridge (U.K.) 1988.
- [12] P.Schuster, *Physica Scripta* **35**(1987) 402.
- [13] J.Hofbauer, *Nonlinear Analysis. Theory, Methods & Applications* **5**(1981)
1003.
- [14] S.Smale, *J.Math.Biol.***3**(1976) 5.
- [15] A.Arneodo, P.Coullet and C.Tresser, *Physics Letters* **79A**(1980) 259.
- [16] A.Arneodo, P.Coullet, J.Peyraud and C.Tresser, *J.Math.Biol.***14**(1982) 153.
- [17] R.R.Vance, *Amer.Natur.***112**(1978) 797.
- [18] M.E.Gilpin, *Amer.Natur.***113**(1979) 306.
- [19] J.F.C.Kingman, *Mathematics of genetic diversity*. CBMS NSF Regional
Conf.Ser.in Appl.Math.Vol.34. SIAM Philadelphia (Penn.) 1980.
- [20] J.F.C.Kingman, *J.Appl.Prob.***15**(1978) 1.

- [21] P.Schuster, K.Sigmund and R.Wolff, *J.Math.Analysis and Applications* **78**(1980) 88.
- [22] P.Schuster, P.Stadler, W.Schnabl and C.Forst, *Dynamics of nonlinear autocatalytic reaction networks*. Akademie-Verlag, Berlin 1990
- [23] J.Guckenheimer and P.Holmes, *Nonlinear oscillations, dynamical systems and bifurcations of vector fields*. Springer-Verlag, New York 1983, pp.318-325.
- [24] N.Samardzija and L.D.Greller, *Bull.Math.Biol.***50**(1988) 465.
- [25] C.Grebogi, E.Ott and J.A.Yorke, *Physica* **7D**(1983) 181.
- [26] I.M.Bomze, *Biol.Cybern.***48**(1983) 201.
- [27] P.F.Stadler and P.Schuster, *Bull.Math.Biol.***5***(1990) ***.
- [28] S.Kim, S.Ostlund and G.Yu, *Physica* **31D**(1988) 117.
- [29] J.D.Farmer, E.Ott and J.A.Yorke, *Physica* **7D**(1983) 153.
- [30] G.Bennetin, L.Galgani, A.Giorgilli and J.-M.Strelcyn, *Meccanica* **15**(1980) 9.
- [31] A.Wolf, J.B.Swift, H.L.Swinney and J.A.Vastano, *Physica* **16D**(1985) 285.
- [32] P.Schuster, K.Sigmund and R.Wolff, *J.Differential Equations* **32**(1979) 357.
- [33] J.Hofbauer, P.Schuster and K.Sigmund, *J.Math.Biol.***11**(1981) 155.
- [34] P.Grassberger, *Phys.Lett.***97A**(1983) 227.
- [35] H.G.E.Hentschel and I.Procaccia, *Physica* **8D**(1983) 453.
- [36] T.C.Halsey, M.H.Jensen, L.P.Kadanoff, I.Procaccia and B.I.Shraiman, *Phys.Rev.A* **33**(1986) 1141.
- [37] M.J.Feigenbaum, *J.Statist.Phys.***46**(1987) 919.
- [38] P.F.Stadler and P.Schuster, *submitted to J.Math.Biol.* (1990).
- [39] J.Hofbauer, P.Schuster, K.Sigmund and R.Wolff, *SIAM J.Appl.Math.* **38**(1980) 282.